Biochemistry **2006,** *45,* 4121−4127

Modification of the Phylloquinone in the A_1 Binding Site in Photosystem I Studied Using Time-Resolved FTIR Difference Spectroscopy and Density Functional Theory[†]

K. M. Priyangika Bandaranayake, Ruili Wang, and Gary Hastings*

Department of Physics and Astronomy, Georgia State University, Atlanta, Georgia 30303

Received October 20, 2005; Revised Manuscript Received January 19, 2006

ABSTRACT: A phylloquinone molecule (2-methyl-3-phytyl-1,4-naphthoquinone) occupies the A_1 binding site in photosystem I. Previously, we have obtained A_1^-/A_1 FTIR difference spectra using labeled and unlabeled photosystem I particles and proposed assignments for many of the bands in the spectra [Sivakumar, V., Wang, R., and Hastings, G. (2005) *Biochemistry 44,* 1880−1893]. In particular, we suggested that a negative/positive band at 1654/1495 cm^{-1} in A_1^-/A_1 FTIR DS is due to a $\mathrm{C{=}O}$/$\mathrm{C\overset{...}{-}O}$ mode of the neutral/anionic phylloquinone, respectively. To test this hypothesis, we have obtained A_1^-/A_1 FTIR DS for *menG* mutant PS I particles. In *menG* mutant PS I, phylloquinone in the A_1 binding site is replaced with an analogue in which the methyl group at position 2 of the quinone ring is replaced with a hydrogen atom (2-phytyl-1,4-naphthoquinone). In A_1^-/A_1 FTIR DS obtained using *menG* mutant PS I particles, we find that the 1654/1495 cm^{-1} bands are upshifted by ∼6 cm^{-1}. To test if such upshifts are likely for $\mathrm{C{=}O}$/$\mathrm{C\overset{...}{-}O}$ modes of neutral/anionic phylloquinone, we have used density functional theory to calculate the "anion minus neutral" infrared difference spectra for both phylloquinone and its methyl-less analogue. We have also undertaken calculations in which the $\mathrm{C_4{=}O}$ carbonyl group of phylloquinone and its methyl-less analogue are hydrogen bonded (to a water or leucine molecule). We find that, irrespective of the hydrogen bonding state of the $\mathrm{C_4{=}O}$ group, the $\mathrm{C{=}O}$/$\mathrm{C\overset{...}{-}O}$ modes of neutral/reduced phylloquinone are indeed expected to be upshifted by at least 6 cm^{-1} upon replacement of the methyl group at position 2 with hydrogen. The calculations also suggest that certain $\mathrm{C{=}C}$/$\mathrm{C\overset{...}{-}C}$ modes of neutral/reduced phylloquinone do not shift upon replacement of the methyl group. On the basis of these calculated results, we suggest which bands in the A_1^-/A_1 FTIR DS may be associated with $\mathrm{C{=}C}$/$\mathrm{C\overset{...}{-}C}$ modes of neutral/reduced phylloquinone, respectively.

Recently, we have used time-resolved step-scan FTIR[1] difference spectroscopy (TRSS FTIR DS) to produce A_1^-/A_1 FTIR difference spectra (DS) for intact photosystem I (PS I) particles from *Synechococcus* sp. 7002 (*S. 7002*) and *Synechocystis* sp. 6803 (*S. 6803*) at 77 K (*1*, *2*). A_1^-/A_1 FTIR DS were also obtained using fully deuterated PS I particles from *S. 7002* and uniformly ^{15}N- and ^{13}C-labeled PS I particles from *S. 6803* (*1*). Comparison of A_1^-/A_1 FTIR DS obtained using the nonlabeled and labeled PS I particles allowed us to propose assignments for many of the bands in the DS. In particular, we proposed that bands near 1654(−) and 1495(+) cm^{-1} in the A_1^-/A_1 FTIR DS are due to carbonyl modes of neutral and reduced phylloquinone (PhQ and PhQ^-), respectively.

One way to test these proposed band assignments is to replace the PhQ in the A_1 binding site with a closely related analogue and monitor how the bands shift in A_1^-/A_1 FTIR DS obtained using these altered PS I particles. With this in mind here, we have produced A_1^-/A_1 FTIR DS using *men*G mutant PS I particles. In *men*G mutant PS I, a PhQ analogue with the 2-methyl group replaced with hydrogen occupies the A_1 binding site (*3*). Below we will refer to the PhQ analogue with a hydrogen atom at position 2 as PhNQ (as an abbreviation for 2-phytyl-1,4-naphthoquinone). The loss of this 2-methyl group might be expected to lead to some alteration of the electronic structure of the naphthoquinone (NQ) headgroup, which in turn will lead to frequency shifts of some of the bands in the A_1^-/A_1 FTIR DS. Unfortunately, the frequency shifts that might be expected for molecular groups of PhQ and PhQ^- upon loss of the methyl group are not easily predicted.

Recently, we have been using density functional theory (DFT) to calculate the vibrational properties of PhQ and PhQ^- molecules in the gas phase (*4*). We were able to calculate infrared (IR) absorption spectra and "anion−neutral" IR difference spectra (DS) for PhQ, and we showed

---

[†] This work was supported by the National Research Initiative of the USDA Cooperative State Research Education and Extension Service Grant 2004-35318-14889 to G.H. R.W. was supported by a fellowship from the Molecular Basis of Disease Program at Georgia State University.

* To whom correspondence should be addressed. E-mail: ghastings@gsu.edu. Phone: (404) 249-7525. Fax: (404) 249-7525.

[1] Abbreviations: $\mathrm{C{=}O}$, carbonyl; $\mathrm{C\overset{...}{-}O}$, semiquinone carbonyl; DFT, density functional theory; DS, difference spectrum, spectra, spectroscopic, or spectroscopy; DDS, double-difference spectrum; FTIR, Fourier transform infrared; H, hydrogen atom; NQ, 1,4-naphthoquinone; PS I, photosystem I; PhQ, 2-methyl-3-phytyl-1,4-naphthoquinone (known as phylloquinone or vitamin K_1); PhNQ, 2-phytyl-1,4-naphthoquinone (quinone present in the A_1 site in PS I from the *menG* mutant); *S. 7002*, *Synechococcus* sp. 7002; *S. 6803*, *Synechocystis* sp. 6803; TRSS, time-resolved step-scan; WT, wild type.

10.1021/bi052145u CCC: \$33.50

that these calculated spectra were very similar to experimental spectra of PhQ in solution (*4*). We were also able to accurately calculate ^{18}O isotope-induced band shifts found experimentally for PhQ in solution. The calculated spectra were also useful for assessing the validity of some of the proposed band assignments in A_1^-/A_1 FTIR DS.

To gain some insight into how vibrational mode frequencies of PhQ will shift in PhNQ, here we extend our DFT studies and calculate the vibrational properties of neutral and anion forms of PhQ and PhNQ. Further, in an attempt to more accurately model the quinone in the A_1 binding site in PS I, we also calculate the vibrational properties of PhQ and PhNQ in which the carbonyl oxygen at position 4 ($C_4{=}O$) is hydrogen (H) bonded, either to a water molecule or to the backbone nitrogen of a leucine molecule.

We show experimentally that difference bands we previously assigned to carbonyl modes PhQ and PhQ^- in A_1^-/A_1 FTIR DS are upshifted by ~6 cm^{-1} in corresponding spectra obtained using PS I particles with PhNQ occupying the A_1 site. From DFT calculations, we show that such an upshift is consistent with our proposed band assignments.

MATERIALS AND METHODS

Wild-type (WT) and *men*G mutant trimeric PS I particles were prepared using standard procedures (*3*−*5*). TRSS FTIR experiments with a time resolution of 5 μs, at 77 K, were undertaken as described previously (*1*). Briefly, A_1^-/A_1 FTIR DS were constructed by subtracting photoaccumulated $P700^+/P700$ FTIR DS from time-resolved $P700^+A_1^-/P700A_1$ FTIR DS collected between 0 and 45 μs after a laser flash (*1*).

The vibrational properties for all quinone molecules discussed here are calculated in the gas phase at 298 K using density functional methods. Calculations were undertaken for both the neutral and anion species. All molecular geometry optimizations and vibrational frequency calculations were performed using hybrid DFT methods, employing the B3LYP functional and the 6-31+G(d) basis using Gaussian 03. Calculated frequencies are unscaled. Intensities are calculated for each normal mode. Calculated intensity stick spectra are then convolved with a Gaussian function with a bandwidth of 4 cm^{-1} (*4*). We refer to the resultant spectra simply as absorption spectra.

To calculate the vibrational properties of PhQ and PhNQ, the models shown in panels A and B of Figure 2 were used, respectively, in which the phytyl chain is limited to only the first four carbon atoms. We have shown previously that limiting the phytyl chain in this way in no way impacts the vibrational properties of the NQ ring (*4*).

RESULTS AND DISCUSSION

Figure 1 shows A_1^-/A_1 FTIR DS obtained using wild-type (WT) and *men*G mutant trimeric PS I particles from *S. 6803*. The "*menG* − WT" FTIR double difference spectrum (DDS) is also shown. Several features in the spectra are noteworthy.

First, the positive band at 1415(+) cm^{-1} is unaltered in the *men*G mutant spectrum. Previously, we suggested that the 1415(+) cm^{-1} band was due to a $C \overset{...}{-} C$ mode of PhQ^- (*1*).

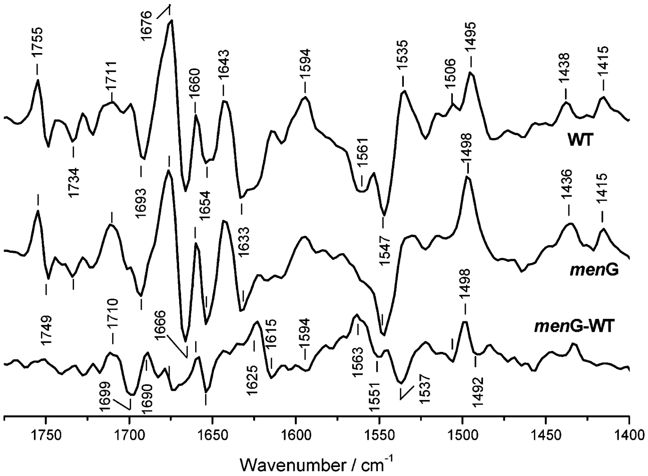

FIGURE 1: A_1^-/A_1 FTIR DS obtained using WT (top) and *men*G mutant (middle) trimeric PS I particles from *S. 6803*. The *menG* − WT FTIR double difference spectrum is also shown (bottom).

Second, the 1495(+) cm^{-1} band in the WT spectrum is upshifted to 1498(+) cm^{-1} in the *men*G mutant spectrum and increases in intensity. The FTIR DDS in Figure 1 suggests that this increase in intensity is due to two components: A positive band near 1506(+) cm^{-1} in the WT spectrum downshifts to near 1498(+) cm^{-1}, and a positive band near 1492(+) cm^{-1} in the WT spectrum upshifts to near 1498(+) cm^{-1}. Previously, we suggested that the positive band at 1495(+) cm^{-1} could be due to a $C \overset{...}{-} O$ mode of PhQ^- (*1*).

Third, a negative band near 1561(−) cm^{-1} in the WT spectrum is downshifted in the *menG* mutant spectrum, possibly to ~1551(−) cm^{-1}. The 1561(−) cm^{-1} band is thought to be an amide II absorption band (*1*). If amide II absorption bands do shift upon mutation, then one might expect that amide I absorption bands will also shift upon mutation. Previously, we suggested that the difference band at 1676(+)/1666(−) cm^{-1} and part of a negative band at 1633(−) cm^{-1} were due to amide I modes (*1*). The difference band at 1676(+)/1666(−) cm^{-1} is not affected by the mutation, while the 1633(−) cm^{-1} band is (Figure 1). The FTIR DDS in Figure 1 could suggest that a negative band at 1625(−) cm^{-1} is downshifted to 1615(−) cm^{-1}.

Fourth, the FTIR DDS in Figure 1 could suggest that a negative band at 1654(−) cm^{-1} upshifts ~6 cm^{-1} to 1660 cm^{-1} upon mutation. Previously, we suggested that the 1654(−) cm^{-1} band could be due to a $C{=}O$ mode of neutral PhQ in the A_1 site that is free from H-bonding (*1*).

In summary, the experimental data in Figure 1, along with our previous interpretation of bands in the spectra (*1*), suggest that carbonyl modes of PhQ and PhQ^- in the A_1 site in PS I upshift by as much as 6 cm^{-1} when PhNQ occupies the A_1 binding site. In addition, at least one of the $C \overset{...}{-} C$ modes of PhQ^- is unaffected by the replacement.

Upon replacement of PhQ with PhNQ, it is not entirely clear what kind of frequency shifts might be expected for the $C{=}O$ and $C{=}C$ modes of PhQ and PhQ^-. We now present a computational investigation of what kind of frequency shifts might be expected for these modes upon exchange.

Figure 2 shows the calculated optimized neutral structure of the (A) PhQ and (B) PhNQ models used in our calcula-

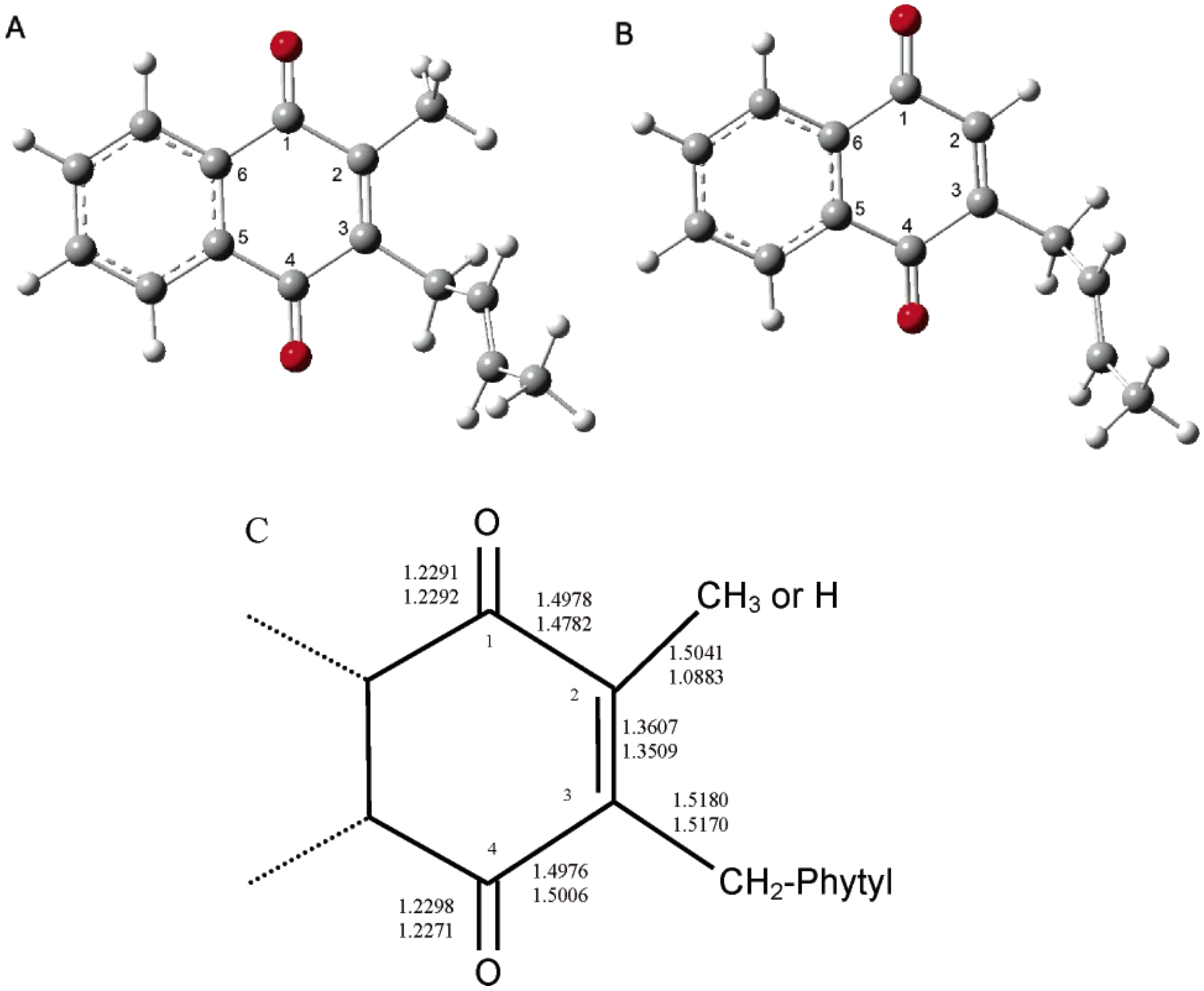

FIGURE 2: Structure and atomic numbering of the (A) PhQ and (B) PhNQ models used in DFT calculations. The structures were optimized using the B3LYP/6-31+G(d) method. In panel A, part of the IUPAC numbering scheme is also shown. In panel C, some of the calculated bond lengths for the quinonic neutral PhQ (top numbers) and PhNQ (bottom numbers) are shown. The part of the NQ ring containing the carbonyl groups (shown in panel C) will be called the quinonic (q) part of NQ. The other fused ring of NQ (not shown in panel C) will be called the aromatic (a) ring.

tions. Part of the IUPAC numbering scheme is also shown. Using the models in panels A and B of Figure 2, we investigate computationally how the substituent attached at C_2 impacts the vibrational structure of PhQ and PhQ^-. The optimized bond lengths calculated for the quinonic part of the molecules in panels A and B of Figure 2 are listed in the structure in panel C. Upper numbers are for PhQ and lower numbers for PhNQ. Changing the C_2 methyl group to H leads to a 0.01 Å shortening of the $C_2{=}C_3$ bond and a 0.0027 Å shortening of the $C_4{=}O$ bond, with very little change in the $C_1{=}O$ bond.

Figure 3A shows calculated "anion − neutral" infrared (IR) difference spectra for the PhQ (dotted) and PhNQ (solid) models shown in panels A and B of Figure 2. In Figure 3A, the three negative bands above ~1640 cm^{-1} are due to the neutral state while the positive bands below ~1570 cm^{-1} are due to the anion radical. The PhQ model in Figure 2A contains 31 atoms. There are therefore 87 normal modes of vibration for this molecule. Most of these modes are of low intensity and are not observable in Figure 3A, and they will not be observable in experimental FTIR DS. The modes that give rise to the prominent bands in Figure 3A are the ones most likely to be observable experimentally, and it is only these modes we will consider here. The most prominent bands in Figure 3A and their mode assignments are listed in Table 1. The calculated shifts in frequency when the C_2 methyl group is replaced with H are also listed in Table 1.

For neutral PhQ, the concerted asymmetric stretching of both C=O modes is calculated to occur at 1721 cm^{-1} and downshift 187 cm^{-1} to 1534 cm^{-1} upon anion formation (Table 1 and Figure 3A). For neutral PhQ, the $C_2{=}C_3$ stretching vibration is calculated to occur at 1666 cm^{-1} and downshift 109 cm^{-1} to 1557 cm^{-1} upon anion formation (Table 1). Pictorial representations of the C=C and C=O modes of PhQ and PhQ^- have been presented previously (*4*). Mode assignments were established by visual inspection of animations of the molecular modes generated using Gaussview. An animation of the 1721 cm^{-1} asymmetric C=O vibration of neutral PhQ is presented in the Supporting Information. Normal modes can be very complex, and only the most prominent molecular group vibrations are listed in Table 1, as described previously (*4*).

Calculated vibrational frequencies are generally higher than experimentally observed frequencies, with no single scaling

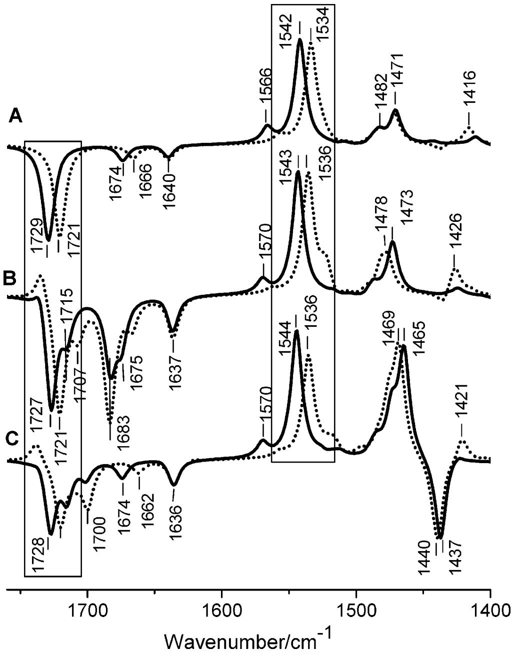

FIGURE 3: (A) Calculated IR difference spectra (anion minus neutral) for the PhQ (···) and PhNQ (—) models shown in Figure 2. (B) Calculated anion minus neutral IR difference spectra for PhQ (···) and PhNQ (—) in the presence of a water molecule, as shown in Figure 4A,B. (C) Calculated anion minus neutral infrared difference spectra for PhQ (···) and PhNQ (—) in the presence of a leucine molecule, as shown in Figure 4C,D. The bands within the solid rectangles are considered in detail in this paper.

factor being directly applicable (*6*). In our DFT studies, we are primarily interested in vibrational frequency changes that occur upon mutation, isotope labeling, or anion formation, and we have shown previously that frequency differences are accurately calculated without scaling. We have therefore chosen not to scale the calculated vibrational frequencies.

Our hypothesis is, however, that the 1534−1536(+) cm^{-1} band in Figure 3A−C corresponds to the 1495(+) cm^{-1} band in Figure 1 (top). In addition, we hypothesize that the 1721(−) cm^{-1} band in Figure 3A−C corresponds to part of the 1654(−) cm^{-1} band in Figure 1 (top).

The experimentally observed spectra in Figure 1 contain contributions from protein modes, while the calculated spectra in Figure 3 do not. This explains why the spectra in Figures 1 and 3 look quite different.

The calculations outlined in Table 1 predict that the asymmetric C═O modes of PhQ and PhQ$^-$ will upshift 8 cm^{-1} upon replacement of the C_2 methyl group with H. In addition, quinonic C═C modes will upshift 7−9 cm^{-1}. Aromatic C═C modes of PhQ and PhQ$^-$ will not shift, however.

The calculations outlined in Figure 3A and Table 1 do not model possible hydrogen bonding interactions that may occur for PhQ in the A_1 site in PS I. For example, for PhQ in PS I the C_4═O group is H-bonded to leucine at position 722 on *PsaA* (leucine at position 706 on *PsaB*) (*1*, *7*). That is the carbonyl oxygen atom adjacent to the phytyl chain is H-bonded to the peptide NH group of a leucine residue. The distance between the nitrogen and oxygen atoms is 2.69 Å (see Figure 1A in ref *1*). In an attempt to model this H-bonding interaction computationally, we have introduced a water molecule, or a leucine molecule, close to the carbonyl oxygen atom, as shown in Figure 4A−D. The distances between atoms for neutral and reduced PhQ and PhNQ in the presence of the various H-bond donors are given in Table 2.

Panels B and C of Figure 3 shows calculated "anion − neutral" IR DS for the PhQ models shown in panels A and B and panels C and D of Figure 4, respectively. The most prominent bands in panels B and C of Figure 3 and their mode assignment are listed in Table 3. The calculated shifts in vibrational frequency upon replacement of the C_2 methyl group with H are also listed in Table 3.

Upon H-bonding, the vibrational mode frequencies are similar. However, the mode composition is quite different. For isolated neutral PhQ, the 1721 cm^{-1} mode is a concerted asymmetric stretching of both C═O groups (see the Supporting Information file I for an animation of the 1721 cm^{-1} mode of PhQ). For PhQ in the presence of H_2O or leucine, however, the ∼1721 cm^{-1} mode is due predominantly to the C_1═O stretching vibration (see Supporting Information File II for an animation of the 1721 cm^{-1} mode of PhQ in the presence of H_2O).

For neutral PhQ, in the absence of a H-bond donor, the symmetric stretching of both C═O modes occurs at 1717 cm^{-1}, with very low intensity. For PhQ in the presence of H_2O or leucine, the C_4═O stretching vibration occurs at 1707 or 1709 cm^{-1} and is coupled to a H_2O or NH_2 "scissoring" vibration, respectively (Table 3). High-intensity modes at 1683/1700 cm^{-1} for neutral PhQ in the presence of water or leucine are also calculated (dotted curves in panels B and C of Figure 3) and are due mainly to H_2O/NH_2 scissoring vibrations, respectively, with minor coupling to the C_4═O stretching vibration (Table 3).

The calculations clearly predict that the H-bonding interaction introduced by the water or leucine molecule uncouples the C═O vibrations of neutral PhQ. Such an uncoupling also occurs for PhQ$^-$, where the 1534(395) cm^{-1} band splits into two bands at 1536 and 1523 cm^{-1} for PhQ$^-$ in the presence of a water molecule (Table 3). The 1536 cm^{-1} band is due mainly to a C_1═O stretching vibration, with significant coupling to the C_4═O vibration. The 1523 cm^{-1} band is due mainly to a C_4═O stretching vibration, with some coupling to the C_1═O vibration.

The main purpose of this paper is not to discuss in detail changes in mode frequency and composition that occur for

Table 1: Approximate Mode Assignments for PhQ and PhQ$^-$ and Its Methyl-less Analogue (PhNQ)[a]

mode	PhQ	PhNQ	Δν	mode	PhQ$^-$	PhNQ$^-$	Δν
ν(C═O), *as*	1721 (369)	1729 (355)	8	ν(C┄O), *as*	1534 (395)	1542 (418)	8
$\nu(C_2═C_3)$, *q*	1666 (52)	1673 (61)	7	$\nu(C_2┄C_3)$, *q*	1557 (31)	1566 (60)	9
ν(C┄C), *a*	1640 (64)	1640 (64)	0	ν(C┄C), δ(C−H)	1483 (46)	1483 (42)	0
				ν(C┄C), δ(C−H)	1471 (112)	1471 (129)	0

[a] The calculated shift in frequency of the modes upon replacement of the C_2 methyl group with H is also listed. The intensity of each vibrational mode is shown in parentheses. Abbreviations: *a*, aromatic; *as*, asymmetric; *q*, quinone ring.

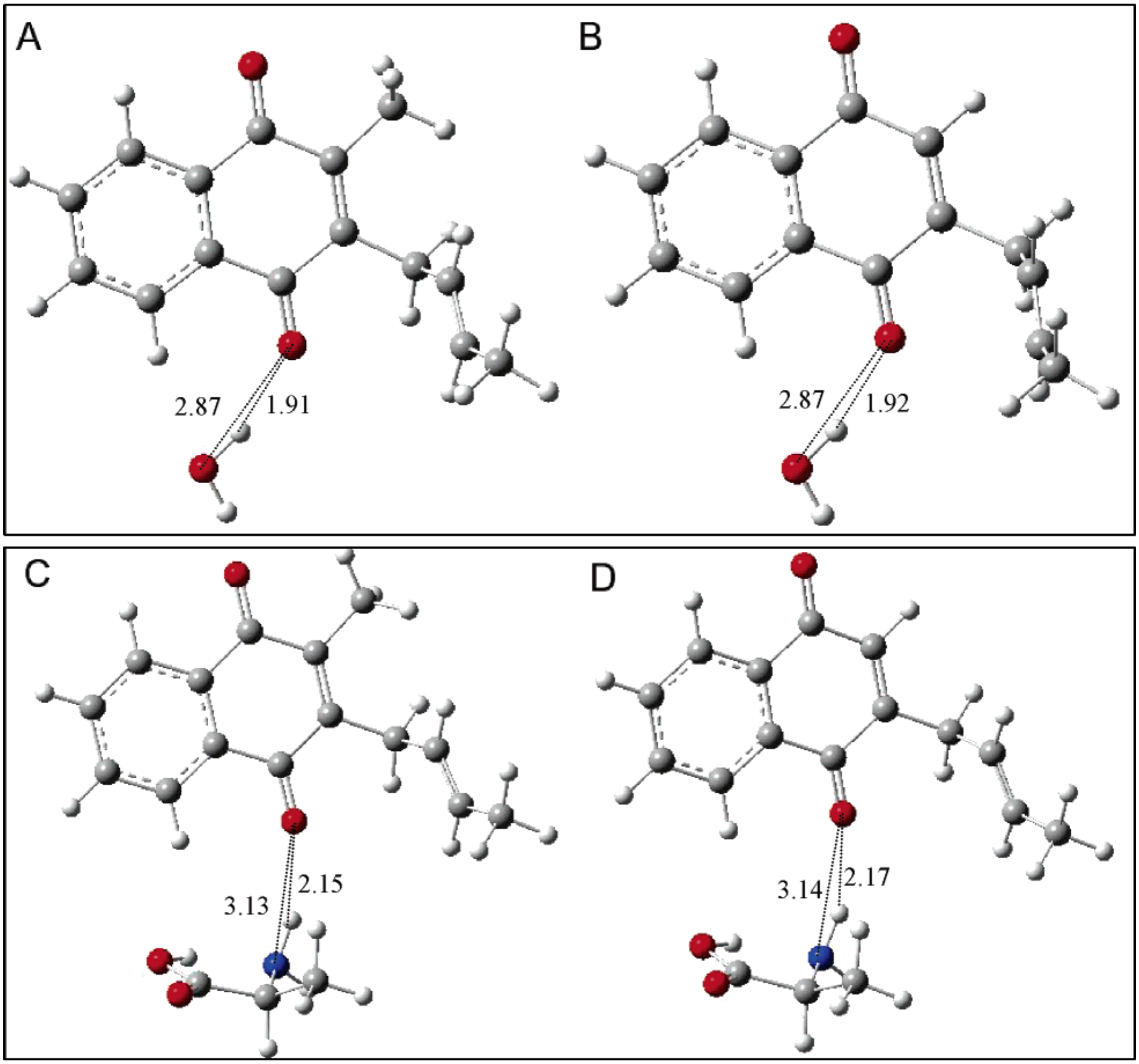

FIGURE 4: Structure of (A and C) PhQ and (B and D) PhNQ in the presence of a water (A and B) or leucine (C and D) molecule. These molecules are used to simulate a possible H-bond to the quinone C_4═O group. Distances are in angstroms.

Table 2: Calculated Distances between the H, N, or O Atoms of the Hydrogen Bond Donor to the Carbonyl Oxygen Atom of Neutral and Reduced PhQ and PhNQ[a]

		distance (Å)			
	bond	PhQ	PhQ^-	PhNQ	$PhNQ^-$
H_2O	H−O	1.91	1.77	1.92	1.77
	O−O	2.87	2.75	2.87	2.76
leucine	H−O	2.15	1.87	2.17	1.86
	N−O	3.13	2.89	3.14	2.88
in PS I	N−O	2.69			

[a] Some of these distances are also shown in Figure 4. The distance between the leucine backbone nitrogen and the carbonyl oxygen of PhQ found using the PS I crystal structure is also listed.

PhQ upon hydrogen bonding. Rather, the purpose is to show that H-bonding of PhQ has little impact on the extent of changes in mode frequency that occur when the C_2 methyl is replaced with hydrogen.

With this in mind, the calculated IR DS in Figure 3A−C share many similarities, and several observations are noteworthy:

(1) For PhQ/PhQ^-, in the absence of a water or leucine molecule, the asymmetric C═O/C$\overset{-}{\cdots}$O mode frequency is upshifted 8/8 cm^{-1}, respectively, upon replacement of the C_2 methyl group with H (Table 1 and boxed region in Figure 3A).

For PhQ/PhQ^- in the presence of a water molecule, the C_1═O mode upshifts 6/7 cm^{-1} upon replacement of the C_2 methyl group with H, respectively (Table 3 and boxed regions in Figure 3B).

For PhQ/PhQ^- in the presence of a leucine molecule, the C_1═O mode upshifts 8/8 cm^{-1} upon replacement of the C_2 methyl group with H, respectively (Table 3 and Figure 3C).

For the H-bonded C_4═O mode, an upshift of 6−8 cm^{-1} is also found for the neutral or anion species upon replacement of the C_2 methyl group (Table 3).

Therefore, in all cases, independent of the H-bonding state of the C_4═O group of PhQ, replacement of the C_2 methyl group of PhQ with H leads to a 6−8 cm^{-1} upshift of both the C_1═O and C_4═O mode frequencies.

Table 3: Approximate Mode Assignments for PhQ and PhQ^- in the Presence of a Water or Leucine Molecule that Can Form a H-Bond to $C_4{=}O$[a]

	PhQ + H_2O	PhNQ + H_2O	$\Delta\nu$		PhQ + Leu	PhNQ + Leu	$\Delta\nu$
$\nu(C_1{=}O)$	1721 (235)	1727 (276)	6	$\nu(C_1{=}O)$	1720 (259)	1728 (286)	8
$\nu(C_4{=}O)$, $\delta(H_2O)$	1707 (65)	1715 (85)	8	$\nu(C_4{=}O)$, $\delta(NH_2)$	1709 (54)	1715 (143)	6
$\delta(H_2O)$	1683 (246)	1683 (167)	0	$\delta(NH_2)$		1701 (64)	
$\nu(C_2{=}C_3)$	1667 (54)	1675 (99)	7	$\nu(C_2{=}C_3)$	1662 (47)	1674 (69)	12
$\nu(C\overset{\cdots}{-}C)$, *a*	1636 (83)	1637 (86)	1	$\nu(C\overset{\cdots}{-}C)$, *a*	1636 (103)	1636 (105)	0

	PhQ^- + H_2O	$PhNQ^-$ + H_2O	$\Delta\nu$		PhQ^- + Leu	$PhNQ^-$ + Leu	$\Delta\nu$
$\nu(C_1{=}O)$	1536 (400)	1543 (492)	7	$\nu(C_1{=}O)$[b]	1536 (408)	1544 (513)	8
$\nu(C_4{=}O)$	1523 (99)						
$\nu(C_2\overset{\cdots}{-}C_3)$[c]	1563 (13)	1570 (53)	7	$\nu(C_2\overset{\cdots}{-}C_3)$[c]	1557 (19)	1570 (58)	13
$\nu(C\overset{\cdots}{-}C)$, *a*	1482 (78)	1486 (40)	4	$\nu(C\overset{\cdots}{-}C)$, *a*	1484 (50)	1485 (54)	1

[a] The approximate mode assignments for PhNQ and $PhNQ^-$ in the presence of a water or leucine molecule are also given. The calculated frequency shifts (for quinones in the presence of a water or leucine molecule) upon replacement of the C_2 methyl group with H are also listed. These shifts should be compared to the corresponding shifts in Table 1. [b] Also contains a contribution from the $C_4{=}O$ mode. [c] Also contains a contribution from aromatic ring C=C modes.

(2) For isolated PhQ/PhQ^-, the $C_2{=}C_3/C_2\overset{\cdots}{-}C_3$ stretching mode at 1666/1557 cm^{-1} is upshifted by 7/9 cm^{-1}, respectively, upon replacement of the C_2 methyl group with H (Table 1). In addition, the intensity of the $C\overset{\cdots}{-}C$ mode of PhQ^- approximately doubles upon replacement of the C_2 methyl group with H. However, it should be noted that the $C_2\overset{\cdots}{-}C_3$ mode of PhQ^- is approximately an order of magnitude less intense than the $C_1\overset{\cdots}{-}O$ mode of PhQ^- (Table 1).

For PhQ/PhQ^- in the presence of a water molecule, the $C_2{=}C_3/C_2\overset{\cdots}{-}C_3$ stretching mode at 1667/1563 cm^{-1} is upshifted by 7/7 cm^{-1}, respectively, upon replacement of the C_2 methyl group with H (Table 3). The intensity of the $C_2\overset{\cdots}{-}C_3$ mode of PhQ^- also increases by a factor of 4 upon replacement of the C_2 methyl group with H. However, again, the $C_2\overset{\cdots}{-}C_3$ mode is approximately an order of magnitude less intense than the $C_1\overset{\cdots}{-}O$ mode (Table 3).

For PhQ/PhQ^-, in the presence of a leucine molecule, the $C_2{=}C_3/C_2\overset{\cdots}{-}C_3$ stretching mode at 1662/1557 cm^{-1} is upshifted by 12/13 cm^{-1}, respectively, upon replacement of the C_2 methyl group with H (Table 3). The intensity of the $C_2\overset{\cdots}{-}C_3$ mode of PhQ^- also increases by a factor of 4 upon replacement of the C_2 methyl group with H. However, again, the $C_2\overset{\cdots}{-}C_3$ mode is still approximately an order of magnitude less intense than the $C_1\overset{\cdots}{-}O$ mode (Table 3).

(3) The band due to aromatic $C\overset{\cdots}{-}C$ vibrations of neutral PhQ (in the absence of a water or leucine molecule) at 1640 cm^{-1} or the band due to aromatic $C\overset{\cdots}{-}C$ vibrations of PhQ^- at 1471 cm^{-1} is unaffected by replacement of the C_2 methyl group with H (Table 1). This observation is roughly the same for PhQ in the presence of a water or leucine molecule (Table 3).

In summary, three important observations from the calculations, independent of the presence or absence of a hydrogen bond donor, are that (1) the $C{=}O/C\overset{\cdots}{-}O$ and quinonic $C{=}C/C\overset{\cdots}{-}C$ modes of PhQ/PhQ^- are expected to be upshifted by at least 6 cm^{-1} in the *menG* mutant, (2) the band associated with the $C\overset{\cdots}{-}O$ mode of PhQ^- is an order of magnitude more intense than the band associated with the $C\overset{\cdots}{-}C$ mode of PhQ^-, and (3) aromatic $C\overset{\cdots}{-}C$ modes of PhQ/PhQ^- appear not to shift upon replacement of the C_2 methyl group with H. These three calculated predictions will now be related to the experimental data in Figure 1.

Previously, we tentatively suggested that the positive band at 1415 cm^{-1} in the WT spectrum in Figure 1 is due to a $C\overset{\cdots}{-}C$ mode of PhQ^- (*1*). We find that the 1415 cm^{-1} band is unaltered in the *menG* mutant A_1^-/A_1 FTIR DS. This observation, along with the calculations outlined in Tables 1 and 3, supports the idea that the 1415 cm^{-1} band in the WT spectrum in Figure 1 is due to an aromatic $C\overset{\cdots}{-}C$ mode of PhQ^-.

In Figure 1, the highest-intensity band in the anion region appears at 1495 cm^{-1}. Part of this band is upshifted by ∼3 cm^{-1} and increases in intensity in the *menG* mutant spectrum. The FTIR DDS in Figure 1 suggest that these features are partly due to a positive band at ∼1492 cm^{-1} upshifting ∼6 cm^{-1} upon mutation. Such features are compatible with the calculations outlined in Figure 3. In Figure 3A (dotted line), the highest-intensity positive band occurs at 1534 cm^{-1} and is due to the combined asymmetric stretching of both $C\overset{\cdots}{-}O$ groups of PhQ^-. Clearly, this band is upshifted by 8 cm^{-1} and increases in intensity by nearly 20% upon replacement of the C_2 methyl group of PhQ with H. The calculated spectra for isolated PhQ and PhNQ (Figure 3A) therefore reproduce well the trends observed in the experimental spectra.

When the $C_4{=}O$ group of PhQ is H-bonded to either a water or a leucine molecule, the highest-intensity anion band is at ∼1536 cm^{-1} (Figure 3B,C) and is due predominantly to a $C_1{=}O$ vibration. Most importantly, the 1536 cm^{-1} band is upshifted by 7−8 cm^{-1} and increases in intensity by nearly 20% upon replacement of the C_2 methyl group of PhQ with H. Thus, the calculated spectra for H-bonded PhQ^- and $PhNQ^-$ also reproduce well the trends observed in the experimental spectra.

The positive band at 1438 cm^{-1} in WT FTIR DS in Figure 1 appears to have broadened and possibly downshifted by ∼2 cm^{-1}. Since the 1438 cm^{-1} band is downshifted slightly in the mutant spectrum, our calculations suggest that it is not due to a $C\overset{\cdots}{-}O$ mode of PhQ^-. It may, however, be due to an aromatic $C\overset{\cdots}{-}C$ mode of PhQ^-.

Previously, we suggested that the negative band at 1654 cm^{-1} in the WT spectrum in Figure 1 is due to a C=O mode of neutral PhQ that is free from H-bonding (the $C_1{=}O$ mode) (*1*). The FTIR DDS in Figure 1 suggests that a band at 1654 cm^{-1} in the WT FTIR DS is upshifted by 6 cm^{-1} upon mutation. The calculated frequency upshift for the $C_1{=}O$ mode is also 6 cm^{-1} (Table 3 and Figure 3B,C). Therefore, the calculated spectra support the hypothesis that the 1654 cm^{-1} band in WT FTIR DS in Figure 1 is due to the $C_1{=}O$ mode of PhQ that is free from H-bonding.

CONCLUSIONS

Vibrational mode frequency calculations for PhQ in the gas phase have been undertaken previously. Here we have extended these calculations to include an asymmetric H-bond to only one of the quinone carbonyl groups. In this way, we more accurately model the PhQ that occupies the A_1 binding site in PS I. For isolated PhQ, only the asymmetric vibration of the $C_1{=}O$ and $C_4{=}O$ groups is IR active. When the $C_4{=}O$ group is H-bonded, the $C_1{=}O$ and $C_4{=}O$ modes "split". The H-bonded $C_4{=}O$ mode moves to lower frequency and is a factor of ~3.6 less intense than the $C_1{=}O$ mode.

DFT calculations were also undertaken for PhNQ. The calculations show that the C═O modes of PhQ and PhQ^- will be upshifted by 6−8 cm^{-1} upon replacement of the C_2 methyl group with H. These calculated assignments correlate very well with experimental observations and our previously proposed assignment of bands in A_1^-/A_1 FTIR DS. The DFT calculations, in combination with experimental spectra for WT and mutant PS I particles, therefore strongly support some of our previously proposed assignments for bands in A_1^-/A_1 FTIR DS.

ACKNOWLEDGMENT

menG mutant PS I particles were a gift from Professor John Golbeck.

SUPPORTING INFORMATION AVAILABLE

Animation of the 1721 cm^{-1} vibration of neutral PhQ in the absence of H-bonding species (Supporting Information file I) and animation of the 1721 cm^{-1} vibration of neutral PhQ in the presence of a water molecule (Figure 4A) (Supporting Information file II). This material is available free of charge via the Internet at http://pubs.acs.org.

REFERENCES

1. Sivakumar, V., Wang, R., and Hastings, G. (2005) A_1 reduction in intact cyanobacterial photosystem I particles studied by time-resolved step-scan Fourier transform infrared difference spectroscopy and isotope labeling, *Biochemistry 44*, 1880−1893.
2. Sivakumar, V., Wang, R., Johnson, T., and Hastings, G. (2005) A_1 Reduction in Intact Cyanobacterial Photosystem I Studied Using Time-resolved Step-scan Fourier Transform Infrared Difference Spectroscopy In Combination With Site Directed Mutagenesis and Quinone Exchange Experiments, in *Photosynthesis: Fundamental Aspects to Global Perspectives* (van der Est, A., and Bruce, D., Eds.) pp 59−60, Alliance Communications Group, Lawrence, KS.
3. Sakuragi, Y., Zybailov, B., Shen, G. Z., Jones, A. D., Chitnis, P. R., van der Est, A., Bittl, R., Zech, S., Stehlik, D., Golbeck, J. H., and Bryant, D. A. (2002) Insertional inactivation of the menG gene, encoding 2-phytyl-1,4-naphthoquinone methyltransferase of *Synechocystis* sp. PCC 6803, results in the incorporation of 2-phytyl-1,4-naphthoquinone into the A_1 site and alteration of the equilibrium constant between A_1 and F-x in photosystem I, *Biochemistry 41*, 394−405.
4. Bandaranayake, K., Sivakumar, V., Wang, R., and Hastings, G. (2006) Modeling The A_1 Binding Site In Photosystem I. Density Functional Theory For The Calculation Of "Anion − Neutral" FTIR Difference Spectra of Phylloquinone, *Vib. Spectrosc.* (in press).
5. Hastings, G., Reed, L., Lin, S., and Blankenship, R. (1995) Excited-state dynamics in photosystem I: Effects of detergent and excitation wavelength, *Biophys. J. 69*, 2044−2055.
6. Rauhut, G., and Pulay, P. (1995) Transferable Scaling Factors for Density-Functional Derived Vibrational Force-Fields, *J. Phys. Chem. 99*, 3093−3100.
7. Jordan, P., Fromme, P., Witt, H. T., Klukas, O., Saenger, W., and Krauss, N. (2001) Three-dimensional structure of cyanobacterial photosystem I at 2.5 angstrom resolution, *Nature 411*, 909−917.

BI052145U